27 May 2010, 4:30 pm - 6:20 pm

# Assessment of Liquefaction-Induced Foundation Soil Deformations

K. Onder Cetin
*Middle East Technical University, Turkey*

Berna Unutmaz
*Kocaeli University, Turkey*

H. Tolga Bilge
*Middle East Technical University, Turkey*


Fifth International Conference on
Recent Advances in Geotechnical Earthquake Engineering and Soil Dynamics
*and Symposium in Honor of Professor I.M. Idriss*
May 24-29, 2010 • San Diego, California

# ASSESSMENT OF LIQUEFACTION-INDUCED FOUNDATION SOIL DEFORMATIONS

**Cetin, K. Onder**
Middle East Technical University
Ankara, Turkey

**Unutmaz, Berna**
Kocaeli University
Kocaeli, Turkey

**Bilge, H. Tolga**
Middle East Technical University
Ankara, Turkey

ABSTRACT

Although there exist some consensus regarding seismic soil liquefaction triggering assessment of free field soil sites, estimating the liquefaction triggering potential beneath building foundations still stays as a controversial and a difficult issue. Assessing liquefaction triggering potential under building foundations requires the estimation of cyclic and static stress state of the soil medium. In the recent studies (e.g. Unutmaz 2008), the cyclic stress ratio corrected for $K_\alpha$ and $K_\sigma$ effects under and adjacent to building foundations subjected to cyclic loading are to be estimated with the help of a series of 2-D and 3-D numerical simulations for different generic cases. A representative and a maximum cyclic stress ratio terms of the soil-structure-earthquake interaction system, denoted as $CSR_{SSEI,rep}$ and $CSR_{SSEI,max}$ respectively was defined as a function of i) ratio of the pre-earthquake fundamental period of the structure and soil ($\sigma$), ii) free field spectral acceleration at the fixed-base period of the structure($S_A$), iii) the peak ground acceleration of the free field soil sites (PGA), and iv) aspect ratio of the structure (h/B). In this paper, the results of the previously mentioned numerical findings have been verified by using case histories documented after 1999 Kocaeli Earthquake, where significant foundation displacements were observed due to liquefaction of the underlying foundation soils. The foundation soil profiles of these case histories generally consist of silty soils, sand-silt mixtures and silt-clay mixtures. Overburden and procedure corrected SPT-N values vary in the range of 2 to 5 blows/30 cm in the upper 5 meters and gradually increases up to a maximum value of 25 blows/30 cm beyond depths of 5 to 8 m's. Overlying structures are mainly 3 to 4 storey, residential buildings with no basements. As the concluding remark, the proposed simplified procedures are shown to predict cyclically-induced foundation settlements accurately within an accuracy factor of two (i.e.: predictions fall within 1:2 and 2:1 limits of the measured settlements).

## INTRODUCTION

Contrary to the free field soil sites, liquefaction assessment of sites with super structures is a controversial and also difficult issue. In this paper, first, the proposed methodology for liquefaction triggering assessment of foundation soils by Unutmaz (2008) will be discussed briefly. Then the methodologies of Cetin et al. (2009) and Bilge and Cetin (2008), which were proposed to estimate strains for coarse- and fine-grained soils, respectively, will be used for validation of the methodology of Unutmaz (2008) through well-documented foundation performance case histories of residential structures founded on liquefiable soils after 1999 Kocaeli earthquake. In addition to calibration and validation efforts, the validity of the following observations based on post earthquake reconnaissance, especially after 1999 Turkey and 2000 Chi-Chi earthquakes, is assessed: i) sand boils were usually observed at the edges of some structures where as no sand boils were observed at free field soil sites with similar soil profiles, (Fig. 1 and Fig. 2), ii) structures located at the end of closely spaced residential building series are more vulnerable to liquefaction-induced bearing capacity loss and corollary tilting (Fig. 3).

This paper tries to assess the behavior of foundation soils from liquefaction assessment and cyclically-induced settlement points. In this content, the paper presents a brief summary of the case histories available, which include the structural and soil properties in addition to the measured settlements at the foundations of structures. These cases are studied in detail and liquefaction triggering potential as well as the settlement predictions is assessed. The whole procedure for a specific case is presented thoroughly for illustration and clarification purposes.

*Fig. 1. Sand boils observed at the edges of structures (photos from nieese.berkeley.edu)*

*Fig. 2. Sand boils observed at the edges of structures (photos from nieese.berkeley.edu)*

*Fig. 3. Structures located at the corners (photos from peer.berkeley.edu)*

## PROPOSED SIMPLIFIED PROCEDURE FOR THE ESTIMATION OF $CSR_{SSEI,rep}$ and $CSR_{SSEI,max}$

Cyclic shear stresses induced on horizontal planes of foundation soils are mainly due to seismic response of the structural and soil masses represented by maximum cyclic base shear, $\tau_{b,\max}$ and $\tau_{soil,\max}$, respectively. Due to complex nature of the interaction, as well as possibly out of phase occurrences of the individual maximum shear, simple sum of these components could be overly conservative. Thus, the contributions (weighting) of these shear components are assessed as given in Equation (1) for both maximum and representative $CSR_{SSEI}$ values:

$$CSR_{eq,SSEI,\alpha=0,\sigma'_v=100kPa}(z) = 0.65 \cdot \frac{\tau_{soil,\max}(z) + f(\sigma)\cdot f\left(\frac{S_A}{PGA}\right)\cdot f\left(\frac{h}{B}\right)\cdot \tau_{b,\max}(z)}{\sigma'_{v,SSI}(z)\cdot K_\alpha(z)\cdot K_\sigma(z)} \quad (1)$$

where, $\sigma'_{v,SSI}(z)$ is the vertical effective stress induced by both the structure and the soil at depth "$z$", and can be practically estimated through simple 2:1 rule, elastic solutions, or more complex 3-D static soil-structure numerical models; $f(\sigma)$, $f(S_A/PGA)$ and $f(h/B)$ are SSEI participation functions, or in simpler terms they model the contribution due to base shear to the induced overall total cyclic shear stresses. In these equations, $S_A$ refers to the spectral acceleration corresponding to the fixed base natural period of the structure, and $PGA$ is the peak ground soil acceleration. The model coefficients for the SSEI participation functions are estimated separately for both representative and maximum $CSR_{eq,SSEI}$ values through maximum likelihood assessments (Cetin et al., 2002). The functional forms that produced the best fit to FLAC-3D results (which were performed for generic soil-structure-earthquake cases) are presented in Table 1, and in Fig. 4 and 5, for $CSR_{SSEI,rep}$ and $CSR_{SSEI,\max}$, respectively. Also in Table 1, standard deviation of the model error, $\sigma_\varepsilon$ is presented.

*Table 1. SSEI participation functions*

| SSEI participation functions | $CSR_{eq,SSEI,rep}$ | | $CSR_{eq,SSEI,\max}$ | |
|---|---|---|---|---|
| | $\theta_1$ | $\theta_2$ | $\theta_1$ | $\theta_2$ |
| $f(\sigma)=\theta_1\exp(-\theta_2\sigma)$ | 14.79 | 0.003 | 2.88 | 0.014 |
| $f\left(\frac{S_A}{PGA}\right)=\theta_1\exp\left(-\theta_2\frac{S_A}{PGA}\right)$ | 0.74 | 0.683 | 1.92 | 0.37 |
| $f\left(\frac{h}{B}\right)=\exp\left(-\theta_1\frac{h}{B}\right)$ | 0.612 | - | 0.122 | - |
| $\sigma_\varepsilon$ | 0.065 | | 0.099 | |

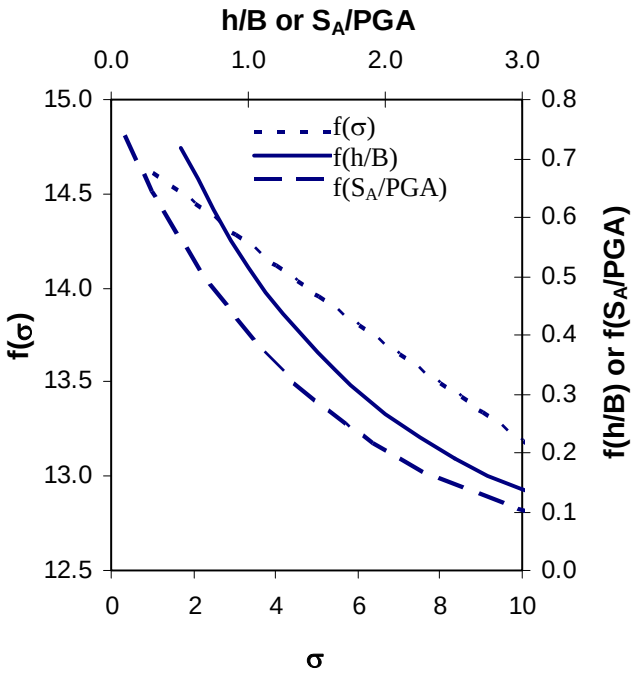


*Fig. 4. SSEI participation functions for $CSR_{SSEI,rep}$*

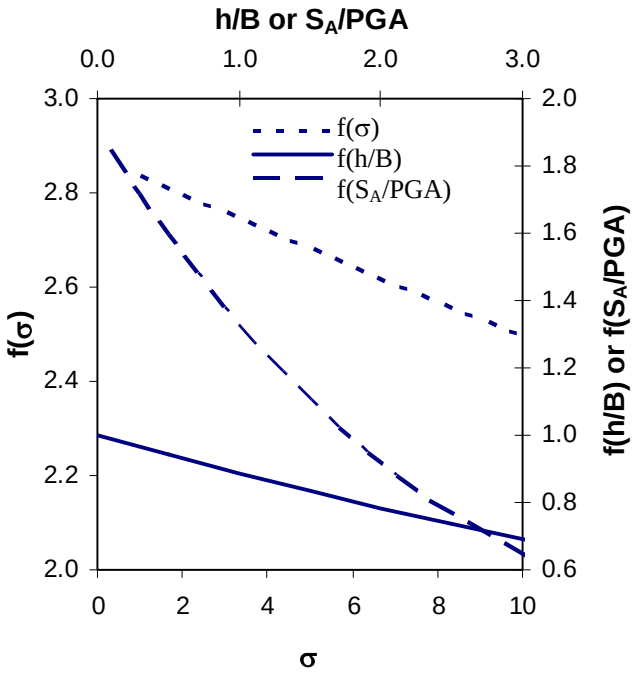


*Fig. 5. SSEI participation functions for $CSR_{SSEI,max}$*

Estimation of $\tau_{b,\max}$ and $\tau_{soil,\max}$

According to NEHRP, the base shear under structures is calculated by using Equation (2).

$$V = C_s(T,\beta)\overline{W} + C_s(T,\beta)\left[W - \overline{W}\right] \qquad (2)$$

where $C_s$ is the dimensionless seismic response coefficient (i.e. spectral acceleration) which depends on the period $(T)$ and the damping $(\beta)$ of the structure. In this equation, $\overline{W}$ represents the generalized or effective weight of the structure when it is vibrating in its natural mode and in simpler terms, a constant value of $\overline{W} = 0.7\,W$ is recommended for typical structures. The second term in Equation (2), however, represents the contribution of higher modes. Period lengthening during shaking significantly affects this second term. For simplicity it is neglected and the maximum base shear is calculated as $V_{b,\max} = 0.8\,W\,S_A$. As discussed earlier, to model the dissipation of base shear with depth, the slope of the shear cone named as the shear stress dissipation factor (=1.6) was estimated by producing a best fit to numerical simulation results. On this basis and inspired by the simplified base shear formulations proposed in various international and national design codes (NEHRP, Eurocode 8, International Building Code 2003, Turkish Earthquake Code 2007), the equivalent structure-induced maximum cyclic base shear beneath a mat foundation was expressed by Equation (3).

$$\tau_{b,\max}(z) = \frac{0.80 \cdot S_A}{(B + 1.6 \cdot z)\cdot(L + 1.6 \cdot z)} \cdot \frac{W_{bldg}}{g} \qquad (3)$$

Cyclic shear stress contributions due to soil mass itself can be estimated consistent with Seed and Idriss (1971) simplified procedure, as given in Equation (4):

$$\tau_{soil,\max}(z) = \frac{a_{\max}}{g} \cdot \gamma_n \cdot z \cdot r_d \qquad (4)$$

Last but not least, to account for the variability in vertical and shear stress conditions under static conditions, $K_\alpha$ and $K_\sigma$ corrections are applied. For the purpose of estimating $K_\sigma$ values, the methodology proposed by Idriss and Boulanger (2006) was adopted. For the estimation of $K_\alpha$ corrections, a representative $\alpha$ field under the structures needs to be estimated first. Static $\alpha$ field is somewhat cumbersome to estimate unless 3-D static soil-structure model results are available. For empirical assessment of the $\alpha$ field, simplified

formulations for representative and maximum $\alpha$ are proposed as given in Equations (5) and (6):

$$\alpha_{rep}(z) = \exp\left(\frac{z-1.48}{-4.36}\right) \times \frac{T_{str}^{-0.12}}{10.03} \times \left(N_{1,60}\right)^{0.04} \quad (5)$$

$$\alpha_{\max}(z) = \exp\left(\frac{z-7.08}{-2.87}\right) \times \frac{T_{str}^{0.45}}{10.36} \times \left(N_{1,60}\right)^{-0.06} \quad (6)$$

where $z$ is the depth from ground surface, $T_{str}$ is the natural period of the structure, $N_{1,60}$ is the representative, overburden and energy corrected representative SPT blow count. For prediction of $K_{\alpha}$, chart solutions proposed by NCEER (1997) were used. The success of the outlined methodology for the estimation of $CSR_{eq,SSEI}$ values is illustrated by Fig. 6 and 7, which compares them by the predictions of FLAC-3D analyses results. The unbiased trend as well as favorable Pearson's product $\left(R^2\right)$ values and almost all data pairs falling into the 2:1 and 1:2 bounds are concluded to be convincing for the success of the proposed methodology.

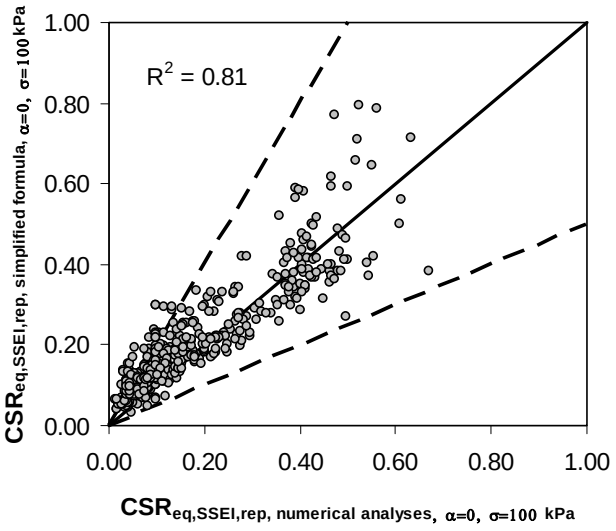


*Fig. 6. Comparison of calculated and predicted $CSR_{eq,SSEI,\ rep}$ values*

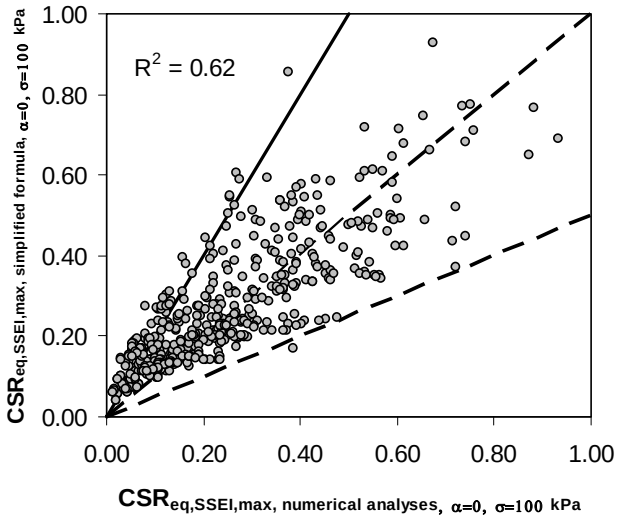


*Fig. 7. Comparison of calculated and predicted $CSR_{eq,SSEI,\ max}$ values*

## CASE HISTORIES AFTER 1999 KOCAELI EARTHQUAKE

After 1999 Kocaeli in Turkey, a number of case histories including the soil and structural characteristics as well as the settlements of the structures have been collected. The case histories comprise of 13 different sites in Kocaeli namely Site A to Site L and more than 25 different buildings resting on these sites. The summary of these case histories is presented in Table 2.

*Table 2. Summary of the available case histories after 1999 Kocaeli earthquake*

| Name of the Bldg | Type of Soil | Structural Properties | | | | Obs. Sett. (cm) |
|---|---|---|---|---|---|---|
| | | B (m) | L (m) | H (m) | $S_A$ (g) | |
| A1 | ML-CH | 9.90 | 11.9 | 14.0 | 0.86 | 10.0 |
| A2 | CH-ML | 13.7 | 17.0 | 14.0 | 0.75 | 50.0 |
| B1 | SP-SM | 5.10 | 20.0 | 14.0 | 0.86 | 20.0 |
| B2 | SP-SM | 6.00 | 23.4 | 14.0 | 0.86 | 0.0 |
| C3 | ML-SP | 19.5 | 20.0 | 14.0 | 0.75 | 17.0 |
| C1 | CH-MH | 19.5 | 20.0 | 14.0 | 0.75 | 17.0 |
| C2 | CL-ML | 19.5 | 20.0 | 14.0 | 0.86 | 20.0 |
| D1 | SW | 9.8 | 11.0 | 14.0 | 0.75 | 60.0 |
| E1 | SP-SM | 12.0 | 17.0 | 14.0 | 0.75 | 20.0 |
| F1 | ML-CL | 7.5 | 13.0 | 11.2 | 0.90 | 50.0 |
| H1 | CH-CL | 10.5 | 14.5 | 11.2 | 0.79 | 18.0 |
| H1 | CH-CL | 9.0 | 18.0 | 11.2 | 0.90 | 2.0 |
| I1 | ML-SP | 9.0 | 18.3 | 11.2 | 0.90 | 10.0 |
| I2 | ML-SP | 13.3 | 14.9 | 16.8 | 0.91 | 12.5 |
| I3 | ML-SP | 14.9 | 14.9 | 16.8 | 0.91 | 15.0 |
| J3 | SM-ML | 22.2 | 24.6 | 14.0 | 0.75 | 20.0 |

*Table 2. cont'd. Summary of the available case histories after 1999 Kocaeli earthquake*

| Name of the Bldg | Type of Soil | Structural Properties | | | | Obs. Sett. (cm) |
|---|---|---|---|---|---|---|
| | | B (m) | L (m) | H (m) | $S_A$ (g) | |
| K2 | ML-SP | 12.6 | 35.6 | 14.0 | 0.75 | 20.0 |
| K2 | ML-SP | 12.6 | 35.6 | 14.0 | 0.86 | 35.0 |
| L1 | ML-SM | 19.1 | 22.1 | 14.0 | 0.86 | 20.0 |
| C2 | CL-ML | 19.5 | 20.0 | 14.0 | 0.75 | 17.0 |
| C2 | ML | 19.5 | 20.0 | 14.0 | 0.75 | 17.0 |
| C4 | ML-SP | 23.4 | 24.0 | 14.0 | 0.75 | 17.0 |
| D1 | ML-SW | 9.8 | 11.0 | 14.0 | 0.86 | 40.0 |
| E3 | SP-SM | 15.0 | 21.6 | 14.0 | 0.75 | 25.0 |

The foundation soil profiles of these case histories generally consist of silty soils, sand-silt mixtures and silt-clay mixtures. Overburden and procedure corrected SPT-N values vary in the range of 2 to 5 blows/30 cm in the upper 5 meters and gradually increases up to a maximum value of 25 blows/30 cm beyond depths of 5 to 8 m's.

Overlying structures are mainly 3 to 6 storey, residential buildings with no basements. The structures were composed of frame elements of beams and columns. Foundation systems were either documented or assumed to be mats. Settlements as well as tilting angles of these buildings were recorded at nearly each building. Details of the case histories, including the lay-out plan, structural dimensions, observed settlements and so on have been presented in Unutmaz (2008)

In the contents of this study, each building (even though settled on the same soil profile) has been considered as a different case and deformation analyses of these structures are performed for each of them individually. Details of calculation steps for an example site (Site I) are also presented for illustration and clarification purposes.

## METHODOLOGY

As mentioned earlier, the case histories documented after 1999 Kocaeli earthquake consist of the building properties (dimensions, number of storey, foundation type and etc.), soil profiles (in terms of field (SPT, CPT and shear wave velocity) and laboratory tests) as well as the foundation settlements and tilting of the structures. In order to validate the methodology proposed for the estimation of the structural-induced cyclic stress ratio values ($CSR_{SSEI}$) by Unutmaz (2008), the deformations are tried to be estimated incorporating these $CSR_{SSEI}$ values into the deformation assessment procedures defined for coarse and fine grained soils. The deformations have been predicted by using the methodologies defined by (i) Cetin et al. (2009) for coarse-grained soils and (ii) Bilge and Cetin (2008) for fine-grained soils. Both formulations estimate the deviatoric and volumetric strains and the profile's settlements are calculated by multiplying these strains with the thicknesses of the corresponding layer and then summing up all these individual components. The variations in the soil profile is eliminated by using the corresponding strain formulation, i.e. if the soil layer consists of both sandy and clayey soils, as generally is, the sandy layers' settlement has been calculated using (i) and the clayey layers' using (ii). A simplified review of these methodologies and how to incorporate them with $CSR_{SSEI}$ in deformation assessments will be presented in the following sections.

i) Deformation assessment of coarse-grained soils

For the deformation assessment of coarse-grained (sandy) soils, the procedure described in Cetin et al. (2009) has been utilized. In that study, the authors have described a maximum likelihood framework for probabilistic assessment of post-cyclic straining of saturated clean sands. They have performed series of stress controlled cyclic triaxial and simple shear tests on laboratory constituted saturated clean sand specimens and also compiled a large number of data from literature. According to their procedure, the deviatoric and volumetric components of strain are calculated separately, multiplied with the corresponding layer thickness and then added up to find the total deformation in the soil profile. Definitions of the maximum shear and volumetric strains are given in Equations (7) and (8), respectively.

$$\gamma_{\max} = \frac{-0.025 \cdot N_{1,60,CS} + \ln\left(CSR_{SS,20,1-D,1atm}\right) + 2.613}{0.001 \cdot N_{1,60,CS} + 0.001} \quad (7)$$

$$\varepsilon_v = 1.879 \cdot \ln\left[\frac{780.416 \cdot \ln(CSR_{SS,20,1-D,1\,atm}) - N_{1,60,CS} + 2442.465}{636.613 \cdot N_{1,60,CS} + 306.732}\right] + 5.583 \quad (8)$$

In these equations, $\gamma_{max}$ and $\varepsilon_v$ represent the maximum double amplitude shear and post-cyclic volumetric strains respectively, both of which are in percent, $N_{1,60,CS,}$ is the overburden and energy corrected SPT-N value for clean sands, $CSR_{SS,20,1\text{-}D,1atm}$ is the CSR value corresponding to a 1 dimensional, 20 uniform loading cycles simple shear test under a confinement pressure of 100 kPa (=1 atm.). In this paper, CSR has been taken as the structural-induced representative or maximum CSR value ($CSR_{SSEI,rep}$ or $CSR_{SSEI,max}$ respectively) and the free field CSR ($CSR_{FF}$) value for different alternatives which will be discussed soon. All of these CSR values are corrected according to the procedure defined in Cetin et al. (2009) to obtain $CSR_{SS,20,1\text{-}D,1atm}$. Details of this CSR calculations and selection of appropriate CSR in settlement assessments will be described in the following sections of this manuscript. In addition to the CSR values, an additional correction factor for depth is also introduced into this formulation in this particular study. Strain values from the upper layers of soil profile are added with a higher weighting factor and the effect of strains diminish with depth. The

formulation for this weighting factor is presented in Equations (9) and (10) for volumetric and deviatoric strains respectively.

$$WF_{vol} = 1 - \theta_{vol} \cdot \left( \frac{d}{B} \right) \quad (9)$$

$$WF_{dev} = 1 - \theta_{dev} \cdot \left( \frac{d}{B} \right) \quad (10)$$

where $\theta_{vol}$ and $\theta_{dev}$ are found to be 0.0 and 0.65 respectively as result of regression analyses. In this formulation $d$ is the depth from the ground surface and $B$ is the width of the structure. The values of weighting factors, $\theta_{vol}$ and $\theta_{dev}$, present that the effect of deviatoric strains on the total settlement diminishes at $d/B < 1.54$. However, volumetric strains effect continues beyond this depth.

ii) Deformation assessment of fine-grained soils

For deformation assessment of fine-grained (clayey) soils, the procedure described in Bilge and Cetin (2008) has been utilized. In that study, the authors have proposed a probabilistically-based semi-empirical model for the assessment of cyclically-induced shear and post-cyclic volumetric (reconsolidation) straining of saturated fine-grained soils. For this purpose, a number of consolidated-undrained, strain-controlled static and stress-controlled cyclic triaxial tests have been performed. After compiling the database, the maximum likelihood methodology is used to develop limit-state models for the estimation of cyclically-induced soil straining. Results are summarized in the form of a semi-empirical stochastic model which enables the estimation of cyclically-induced maximum shear and post-cyclic volumetric straining as a function of liquid limit ($LL$), plasticity index ($PI$), natural moisture content ($w_c$), undrained shear strength ($s_u$), cyclic and static shear stresses ($\tau_{cyc}$ and $\tau_{st}$ respectively). According to that the study, the maximum shear strain (deviatoric strain) is calculated using Equation (11):

$$\gamma_{\max} = \ln 20.17 \frac{22.88^{\left(0.75\frac{w_c}{LL}\right)}}{\ln(PI)} \cdot \frac{0.84 - \sqrt{\left(\frac{\tau_{st}}{s_u} - 0.72\right)^2 + \left(\frac{\tau_{cyc}}{s_u} + 0.60\right)^2}}{-5.2} \quad (11)$$

The volumetric strain is then calculated by Equation (12):

$$\varepsilon_v = 0.28 \cdot \gamma_{\max}^{0.68} \quad (12)$$

As mentioned previously, the case histories in this study include detailed laboratory testing of the samples. These laboratory tests include $w_c$, $LL$ and $PI$ values. However, the $s_u$ values have not been reported for most of the cases. For this reason, the undrained shear strength values required for the analyses have been calculated from the $SPT - N$ values (i.e. $s_u = 5N$). The static and cyclic shear stresses were calculated by multiplying the initial (static) shear stress ratio ($\alpha$) and CSR (either $CSR_{SSEI,rep}$, $CSR_{SSEI.max}$ or $CSR_{FF}$) values with the vertical effective stress respectively. $\alpha$ values are calculated using the procedure defined in Unutmaz (2008), i.e. Equations (5) and (6), and CSR is the corresponding structural-induced cyclic stress ratio which be discussed in detail in the next section.

Shear stresses and shear stress ratios (CSR):

Other than the shear stresses, the remaining variables in Equations 9, 10, 11 and 12, i.e. ($N_{1,60,cs}$, $w_c$, $LL$, $PI$ and $s_u$) can be obtained easily from field or laboratory tests. However, determination of shear stresses and cyclic shear ratio values especially beneath the structures need more attention. For free field cases, shear stresses as well as the CSR values are calculated by using the simplified procedure of Seed and Idriss (1971). However, for the case of foundation soils, there is a conflict about which shear stress or shear stress ratio to be used. In Unutmaz (2008), two different structural-induced CSR values (and accordingly two different shear stresses) have been proposed for foundation soils: $CSR_{SSEI,rep}$ and $CSR_{SSEI,max}$. In this paper, various alternatives and combinations of these stress ratios have been studied in detail and it is tried to determine which shear stress and/or stress ratio dominates the behavior of foundation settlements. For the selection of the suitable values, measured and estimated settlements are compared. For clarification purposes, calculation and selection of the stress ratios will be explained on an example site.

The following section discusses the details of a specific case history and the procedure followed during the determination of the settlements.

AN EXAMPLE CASE: SITE I

One of the cases studied after 1999 Kocaeli Earthquake was Site I, located in Semerciler District, Adapazari, at Cark Avenue. The geographical coordinates of this site is N40.78 E30.39. A general overview for this case is presented in Fig. 8. As can be seen from this figure, closely located, three buildings, Buildings I1, I2 and I3, rest on this site. I1 is a 4 storey whereas the other two are 6 storey residential buildings. The magnitudes of the settlements observed at the edges of the structures are also shown in Fig. 8. The black dots shown in Fig. 8 indicate the locations of the field tests performed which include one standard penetration (SPT) and four cone penetration tests (CPT). As this figure implies, Building I2 has

settled by an amount of 12.5 cm where Building I1 has settled 10 cm and a barely noticeable tilt has been observed in this building. As a particular example, Building I2, whose properties are summarized in Table 3, will be studied in detail. The liquefaction triggering potential of foundation soils, including the estimation of simplified model input parameters will be discussed next, by illustrating the calculation details. The generalized soil profile based on the SPT-I1 is presented in Table 4. The ground water table is located at 0.74 m beneath the soil surface.

*Table 3. Summary of the of building and earthquake properties for Site I*

| | |
|---|---|
| Width of Building I2, $B$ | 13.3 m |
| Length of Building I2, $L$ | 14.9 m |
| Height of Building I2, $H$ | 6 storey, ~16.8 m |
| Period of the structure, $T_{str}$ | ~0.6 sec |
| Moment magnitude, $M_w$ | 7.2 |
| Peak ground acceleration, $PGA$ | 0.40 g |
| Spectral acceleration, $S_A$ (corresponding to structural period of 0.6 seconds) | 0.91 g |

*Table 4. Generalized soil profile (based on SPT-I1)*

| Depth | SPT-N | Type of Soil | $D_R$ | $LL$ | $PI$ | $FC$ | $w_c$ |
|---|---|---|---|---|---|---|---|
| 1.1 | 6 | CH | 74 | 73 | 48 | 99 | 37 |
| 2.2 | 6 | ML | 57 | 29 | 22 | 0 | 20 |
| 3.1 | 4 | ML | 51 | 29 | 22 | 64 | 20 |
| 4.2 | 4 | ML | 51 | 39 | 13 | 89 | 36 |
| 5.0 | 9 | ML | 71 | 53 | 33 | 94 | 42 |
| 6.3 | 10 | CH | 72 | 35 | 22 | 96 | 36 |
| 7.2 | 28 | SP-SM | 95 | 15 | 12 | 8 | 23 |
| 8.0 | 41 | SP-SM | 100 | 15 | 12 | 9 | 21 |
| 9.0 | 43 | SP-SM | 100 | 15 | 12 | 5 | 19 |
| 19.0 | 43 | SP-SM | 100 | 15 | 12 | 5 | 19 |

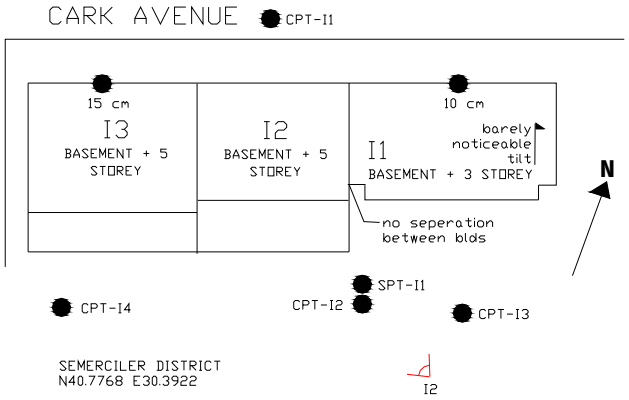


*Fig. 8. A general view of Site I*

Model input parameters

The proposed simplified procedure (Unutmaz, 2008), needs easy to estimate, yet powerful enough parameters to capture the observed response. These parameters are grouped as: i) structural, ii) geotechnical and iii) ground motion related. A summary of these properties (i.e. width, length, period, moment magnitude, spectral acceleration…) for this particular case (Building I2 resting on Site I, SPT – I1) is presented in Table 3. For the purpose of evaluating some earthquake related parameters, one dimensional equivalent linear seismic response analyses were performed. For every case history site, elastic response spectrum corresponding to 5% damping was determined.

Calculation of $CSR_{SSEI,rep}$ and $CSR_{SSEI,max}$

The variables which are not listed in Table 3 can be predicted as stated in preceding section. Some of these values, such as the vertical and shear stresses vary with depth, however the functions of $S_A/PGA$, $h/B$ and σ are constant for a specific site and/or building. The formulation proposed by Unutmaz (2008) for $CSR_{SSEI,rep}$ and $CSR_{SSEI,\max}$ is presented in Equations (13) and (14) respectively.

$$CSR_{SSEI,rep} = \frac{14.77 \cdot \exp\left(\sigma^{-0.01}\right) \times 0.79 \cdot \exp\left(\left(\frac{S_A}{PGA}\right)^{-0.68}\right) \times \exp\left(\left(\frac{h}{B}\right)^{-0.66}\right) \cdot \tau_b + \tau_{soil}}{\sigma_{SSI}} \quad (13)$$

$$CSR_{SSEI,\max} = \frac{2.88 \cdot \exp\left(\sigma^{-0.014}\right) \times 1.92 \cdot \exp\left(\left(\frac{S_A}{PGA}\right)^{-0.37}\right) \times \exp\left(\left(\frac{h}{B}\right)^{-0.122}\right) \cdot \tau_b + \tau_{soil}}{\sigma_{SSI}} \quad (14)$$

The variables used in these equations ($S_A/PGA$, $h/B$ and σ) are listed in Table 5.

*Table 5. Constants for Building I2 of Site I*

| | For $CSR_{SSEI,rep}$ | For $CSR_{SSEI,\max}$ |
|---|---|---|
| $\frac{S_A}{PGA}=2.6$ | $f\left(\frac{S_A}{PGA}\right)=0.14$ | $f\left(\frac{S_A}{PGA}\right)=0.7$ |
| $\frac{h}{B}=1.26$ | $f\left(\frac{h}{B}\right)=0.43$ | $f\left(\frac{h}{B}\right)=0.86$ |
| $\sigma=10.9$ | $f(\sigma)=13.1$ | $f(\sigma)=2.46$ |

Calculation of settlements:

Fig. 9 presents a brief summary of the calculation procedure. As illustrated in this figure, after obtaining the required variables from field and laboratory tests, the deviatoric and volumetric strains are calculated separately for sandy and clayey layers by the corresponding formulations. Then these strains are multiplied with the thicknesses of the layers to predict the layer's settlement. Finally, to estimate the total settlement, the deviatoric and volumetric components for sandy and clayey layers along the soil profile are added up multiplied with different weighing factors (i.e. $\theta_{dev}$ and $\theta_{vol}$ ).Table 6 presents the numerical values of the calculated strains, and settlements for the example case. $K_\alpha$ values in Table 6 have been calculated using the chart proposed by NCEER 1997. $K_\sigma$ values were calculated after Idriss and Boulanger (2006). $r_d$ values are calculated by Cetin and Seed. (2004). $CSR_{FF}$ is calculated by the simplified procedure of Seed and Idriss (1971). $CSR_{SSEI,rep}$, $CSR_{SSEI,\max}$, $\alpha_{rep}$ and $\alpha_{\max}$ are calculated using the procedures defined in Unutmaz (2008).

Volumetric settlement is calculated by multiplying the volumetric strains (Columns 15, 17 and 19) with the thicknesses of the corresponding layer (Column 5) for representative, maximum and free field components respectively. Same operations are also performed for the deviatoric component (Columns 16, 18 and 20) too. Then the two components are added up after multiplying them with the weighing factors $\theta_{dev}=0.01$ and $\theta_{vol}=0.55$ for deviatoric and volumetric components, respectively.

The main goal of this study is to check both the proposed formulations for both strains and cyclic stress ratios represent the real world and to propose a simple tool for foundation settlements specifically after dynamic excitation. For this reason, observed settlements are compared with the estimated settlements.

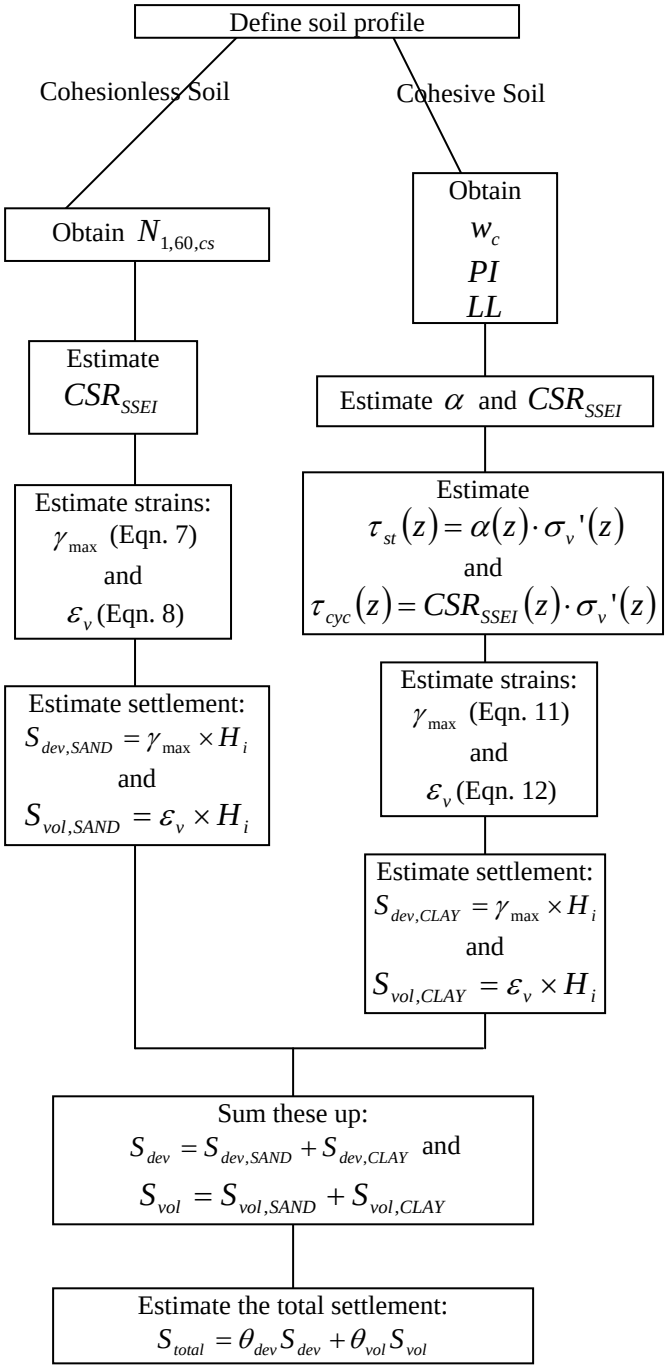


*Fig. 9. Flowchart summarizing analyses steps*

However, as defined earlier, for structural-induced cyclic stress ratio values, there are two different approaches: (i) representative and (ii) maximum $CSR_{SSEI}$. Representative $CSR_{SSEI}$ ($CSR_{SSEI,rep}$) represents the average behavior beneath the structure, whereas the maximum $CSR_{SSEI}$ ($CSR_{SSEI,\max}$) is the maximum value of $CSR_{SSEI}$ along the width of the structure which is generally located at the edges of the structure. In this study, both of these $CSR_{SSEI}$ values are used for prediction of the settlements. Additionally, free

field settlements are predicted using free field $CSR$ values ($CSR_{FF}$) and then these values are subtracted from the former settlements to obtain the differential settlement value. These predictions along with the measured settlements are comparatively presented in Fig. 10 and Fig. 11 for representative and maximum CSR values, respectively.

*Table 6. Calculation Steps for Building I2 of Site I*

| SPT-N | Depth (m) | $CSR_{rep}$ | $CSR_{max}$ | $K_\sigma$ | $\alpha_{rep}$ | $\alpha_{max}$ | $K_\alpha$ | $\tau_{cyc,rep}$ | $\tau_{st,rep}$ | $\varepsilon_{v,rep,}$ Considered | $\gamma_{rep}$ Considered | $\tau_{cyc,max}$ | $\tau_{st,max}$ | $\varepsilon_{v,max,}$ Considered | $\gamma_{max}$ Considered | $\tau_{cyc,FF}$ | $\tau_{st,FF}$ | $\varepsilon_{v,FF,}$ Considered | $\gamma_{FF}$ Considered | Obs. Sett. (cm) | Volumetric Free Field Settlement (cm) | Deviatoric Free Field Settlement (cm) | Volumetric Rep. Settlement (cm) | Deviatoric Rep. Settlement (cm) | Volumetric Max. Settlement (cm) | Deviatoric Max. Settlement (cm) |
|---|---|---|---|---|---|---|---|---|---|---|---|---|---|---|---|---|---|---|---|---|---|---|---|---|---|---|
| 6 | 1.10 | 0.38 | 0.70 | 0.86 | 0.18 | 0.32 | 0.79 | 91 | 2 | 0.70 | 3.75 | 167 | 5 | 1.08 | 7.08 | 3 | 0 | 0.15 | 0.41 | 12.5 | 16 | 102 | 26 | 191 | 31 | 261 |
| 6 | 2.20 | 0.36 | 0.63 | 0.92 | 0.12 | 0.25 | 0.86 | 76 | 3 | 1.14 | 7.65 | 136 | 6 | 1.72 | 13.89 | 7 | 0 | 0.31 | 1.16 | | | | | | | |
| 4 | 3.10 | 0.35 | 0.60 | 0.93 | 0.09 | 0.20 | 0.89 | 70 | 3 | 1.52 | 11.66 | 120 | 7 | 2.24 | 20.41 | 8 | 0 | 0.40 | 1.71 | | | | | | | |
| 4 | 4.20 | 0.34 | 0.57 | 0.94 | 0.07 | 0.17 | 0.87 | 66 | 3 | 2.86 | 28.97 | 108 | 7 | 4.08 | 48.62 | 10 | 0 | 0.81 | 4.66 | | | | | | | |
| 9 | 5.00 | 0.35 | 0.54 | 0.91 | 0.06 | 0.14 | 0.93 | 63 | 3 | 0.96 | 5.97 | 100 | 7 | 1.32 | 9.44 | 16 | 0 | 0.43 | 1.87 | | | | | | | |
| 10 | 6.30 | 0.35 | 0.53 | 0.91 | 0.04 | 0.11 | 0.95 | 62 | 2 | 1.51 | 11.53 | 94 | 6 | 2.00 | 17.31 | 19 | 0 | 0.74 | 4.10 | | | | | | | |
| 28 | 7.20 | 0.35 | 0.51 | 0.83 | 0.04 | 0.09 | 1.00 | 62 | 2 | 1.92 | 16.34 | 90 | 6 | 2.36 | 21.97 | 28 | 0 | 1.35 | 9.77 | | | | | | | |
| 41 | 8.00 | 0.36 | 0.50 | 1.00 | 0.03 | 0.08 | 1.00 | 63 | 2 | 1.31 | 9.39 | 88 | 6 | 1.54 | 11.87 | 34 | 0 | 1.02 | 6.53 | | | | | | | |
| 43 | 9.00 | 0.41 | 0.49 | 0.82 | 0.01 | 0.03 | 1.00 | 75 | 1 | 1.30 | 9.22 | 88 | 3 | 1.42 | 10.49 | 52 | 0 | 1.08 | 7.03 | | | | | | | |

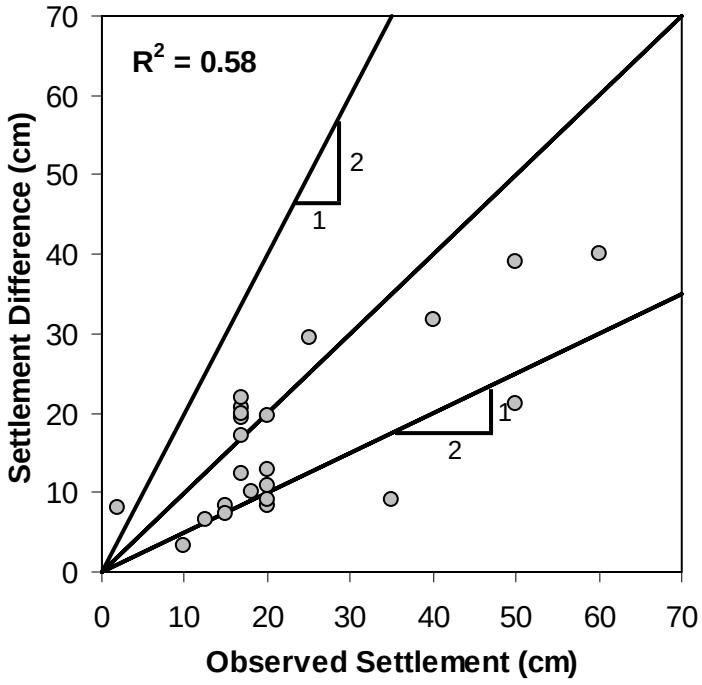


*Fig. 10. Comparison of predicted and observed settlements using* $CSR_{SSEI,rep} - CSR_{SSEI,FF}$

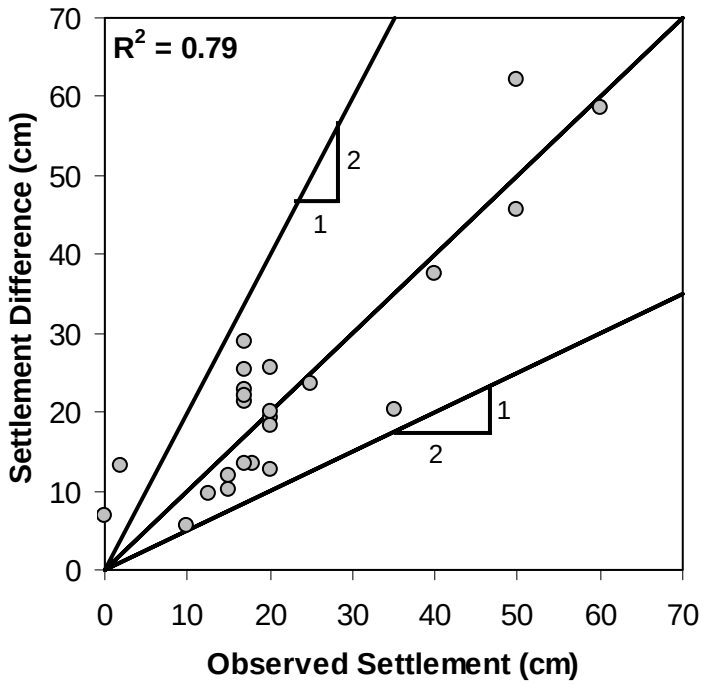


*Fig. 11. Comparison of predicted and observed settlements using* $CSR_{SSEI,\max} - CSR_{SSEI,FF}$

The solid lines in these figures are 45° lines (1:1) and the dashed lines are 1:2 and 2:1 lines. These two graph show that

the estimated settlements match with the observed settlements in the range which can be counted as a good match from geotechnical earthquake engineering point of view. However, the best match between the predicted and observed settlements were obtained by the second item which is calculated by subtracting the free field settlement from the settlement obtained by $CSR_{SSEI,\max}$. This result makes sense as the $CSR_{SSEI}$ gets its highest value at the edges of the structures, and the measured settlements are the relative settlement of the building's edges relative to the free field. As mentioned previously, the volumetric and deviatoric settlements were multiplied with different constants to obtain the total settlement. Below an example calculation is presented (recall that the observed settlement for Building I2 was 12.5 cm):

$$\begin{aligned} \textit{Total Settlement} &= \theta_{vol} \times \left(\varepsilon_{v,\max} - \varepsilon_{v,FF}\right) + \theta_{dev} \times \left(\gamma_{\max} - \gamma_{FF}\right) \\ &= 0.55 \times (31-16) + 0.01 \times (261-102) \\ &= 8.3 + 1.6 \\ &\cong 10\ cm \end{aligned}$$

Although, the portion of volumetric component seems very high at first glance $\left(\theta_{vol} = 0.55 > \theta_{dev} = 0.01\right)$, when it is investigated thoroughly, it can be seen that it constitutes about two thirds of the total settlement as illustrated in Fig. 12.

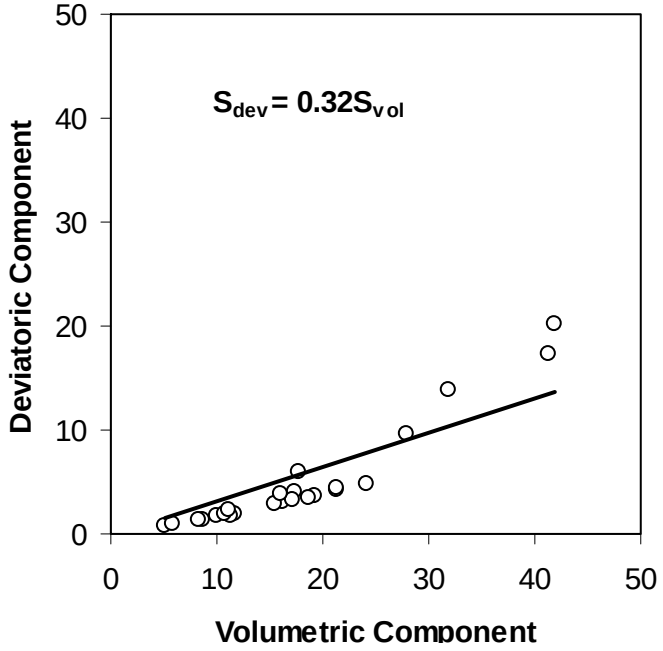


*Fig. 12. Ratio of deviatoric component to the volumetric component*

Figure 13 presents the $\pm 1\sigma_{\varepsilon}$ for all cases and as revealed by this figure, all the settlement values predicted fall within the rage of 1:2 and 2:1 lines.

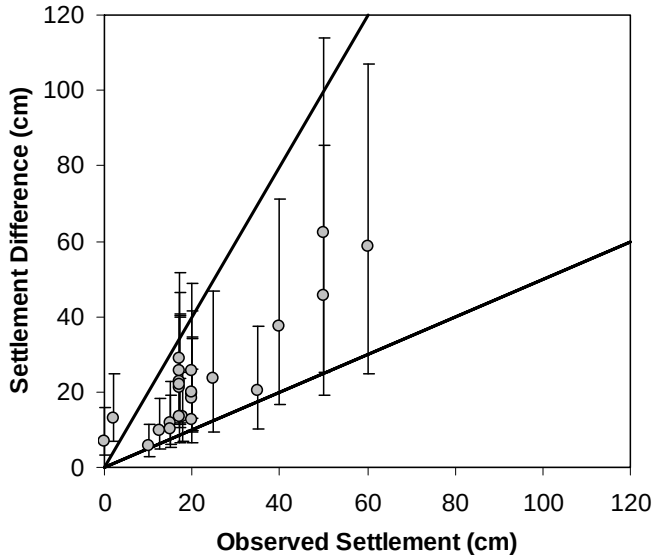


*Fig. 13. Ratio $\pm 1\sigma_{\varepsilon}$ for settlements using $CSR_{SSEI,\max} - CSR_{SSEI,FF}$*

## SUMMARY AND CONCLUSIONS

This paper focused on the validation of the methodology proposed by Unutmaz (2008) using the strain prediction models of Bilge and Cetin (2008) and Cetin et al. (2009) along with the well-documented foundation performance case histories of residential structures founded on liquefiable soils after 1999 Turkey earthquakes. The foundation soil profiles of these case histories generally consist of silty soils, sand-silt mixtures and silt-clay mixtures. Overburden and procedure corrected SPT-N values vary in the range of 2 to 5 blows/30 cm in the upper 5 meters and gradually increases up to a maximum value of 25 blows/30 cm beyond depths of 5 to 8 m's. Overlying structures are mainly 3 to 6 storey, residential buildings with no basements. The structures were composed of frame elements of beams and columns. Foundation systems were either documented or assumed to be mats. Liquefaction triggering performance as well as foundation settlements of the case histories is assessed through the proposed methodology. In addition to calibration and validation efforts, the validity of the following observations based on post earthquake reconnaissance, especially after 1999 Kocaeli and Duzce and 2000 Chi-Chi earthquakes, is assessed: i) sand boils were usually observed at the edges of some structures where as no sand boils were observed at free field soil sites with similar soil profiles, ii) structures located at the end of closely spaced residential building series are more vulnerable to liquefaction-induced bearing capacity loss and corollary tilting. As the concluding remark, the simplified procedure proposed in Unutmaz (2008) is shown to capture almost all of

the behavioral trends and most of the foundation settlement amplitudes.

## REFERENCES


Bilge, H.T., and Cetin, K.O [2008]. “Probabilistic assessment of cyclic soil straining in fine-grained soils.”, Proc. of Geotech. Earthquake Engnrg. and Soil Dynamics IV, GSP 181, Sacramento, CA, USA.

Cetin, K.O., and Seed, R.B. [2004], “Nonlinear Shear Mass Participation Factor (rd) for Cyclic Shear Stress Ratio Evaluation”, J. Soil Dynamics and Earthquake Engrg., Vol. 24, pp. 103-113.

Cetin K.O., Bilge H.T., Wu J., Kammerer A. and Seed R.B., [2009]. “Probabilistic Models for Cyclic Straining of Saturated Clean Sands.” J. Geotech. and Geoenv. Engrg., 135[3], 371-386.

Idriss, I.M., and Boulanger, R.W., [2006]. “Semi-empirical Procedures for Evaluating Liquefaction Potential During Earthquakes.” Soil Dynamics and Earthquake Engrg., 26[2-4], 115-130.

NCEER [1997], “Proceedings of the NCEER workshop on Evaluation of Liquefaction Resistance of Soils.” Edited by Youd, T. L., Idriss, I. M., Technical Report No. NCEER-97-0022, December 31, 1997.

Seed, H.B., Idriss, I.M. [1971], “Simplified Procedure for Evaluating Soil Liquefaction Potential.” J. Soil Mechanics and Foundation Division, 97[SM9], Proc. Paper 8371, 1249 – 1273

Unutmaz, B. [2008], “Assessment of soil – structure – earthquake interaction induced soil liquefaction triggering.” PhD Dissertation, Middle East Technical University, Ankara.